

Article

Investigations on the Solubility of Vortioxetine Based on X-ray Structural Data and Crystal Contacts

Xian-Rui Zhang, Lei Gao, Gui-Yuan He and Chao-Jie Chen *

School of Chemical Engineering and resource recycling, Wuzhou University, Wuzhou 543000, China; zhangyang159246@163.com (X.-R.Z.); gaolei_1008@163.com (L.G.); heguiyuan123@163.com (G.-Y.H.)

* Correspondence: chaojiechen@yahoo.com; Tel.: +86-0774-5828709

Received: 18 September 2019; Accepted: 16 October 2019; Published: 18 October 2019



Abstract: Investigation on the solid-state pharmaceutical chemistry has been known as an intriguing strategy to not only modify the physicochemical properties of drugs but also expand the solid form landscape. Vortioxetine (VOT) is an effective but poorly soluble antidepressant. To improve the solubility of vortioxetine and expand possible solid forms, in this paper, four novel solid forms of vortioxetine with dihydroxybenzoic acids (VOT-23BA, VOT-24BA-TOL, VOT-25BA, and VOT-26BA, 23BA = 2,3-dihydroxybenzoic acid, 24BA = 2,4-dihydroxybenzoic acid, 25BA = 2,5-dihydroxybenzoic acid, 26BA = 2,6-dihydroxybenzoic acid, and TOL = toluene) were synthesized first by a solvent evaporation method and then characterized by single-crystal X-ray diffraction (SCXRD), thermal, and XRD techniques. VOT-24BA-TOL, VOT-25BA, and VOT-26BA, showed similar [2+2] tetrameric R_4^4 (12) hydrogen bonds by acid-piperazine heterosynthon. In the VOT-23BA-H₂O salt, the VOT cation and 23BA anion interacted through protonated piperazine-hydroxyl N-H...O hydrogen bonds, not protonated piperazine-deprotonated carboxylic acid N-H...O hydrogen bonds. Solubility studies were carried out in purified water and it was found that the VOT-23BA-H₂O, VOT-25BA, and VOT-26BA salts exhibited an increase in water compared to pure VOT. The solubility of the stabilized salt formations followed the order of VOT-25BA > VOT-26BA > VOT-23BA-H₂O in purified water.

Keywords: vortioxetine; dihydroxybenzoic acids; salt; crystal structure; solubility

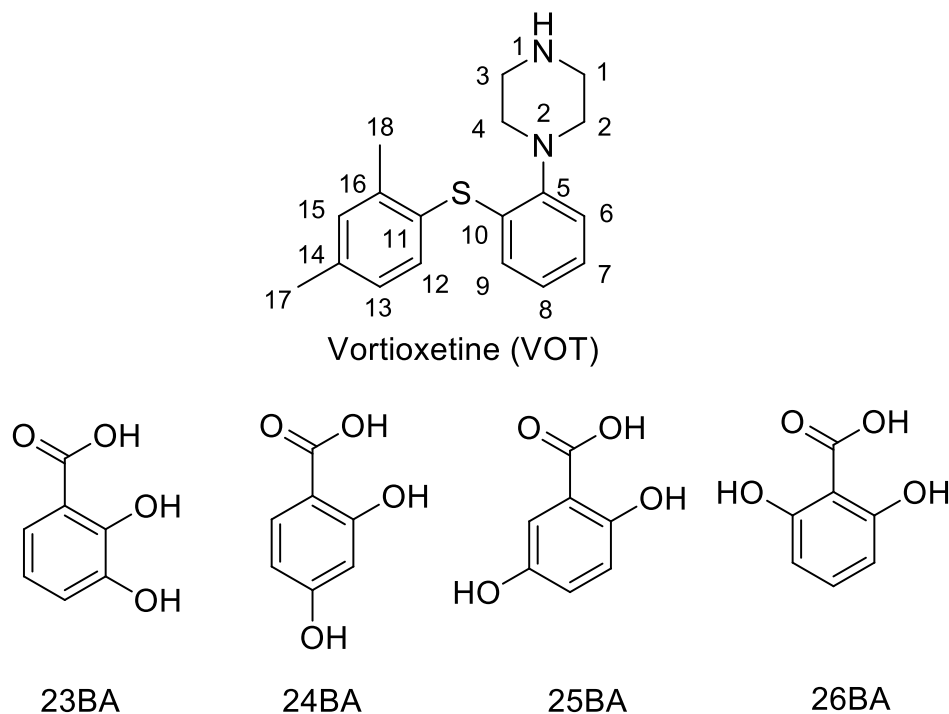
1. Introduction

In recent years, the study of solid-state pharmaceutical chemistry, including cocrystals, salts, polymorphs, and solvates, has been extensively applied in the area of pharmaceutical technology [1–5]. Thus, the design of pharmaceutical solid forms of drugs has become an important step in the pharmaceutical process [6]. Salt formations, in particular, usually improve the physicochemical properties, solubility, and dissolution rate of drugs [7–11]. These advantages are useful for judging whether salt formations can be new API candidates.

Dihydroxybenzoic acids contain two hydroxyl groups and one carboxyl group and have the ability to form complex and robust hydrogen-bond networks [11–20], which are often used as the preferred candidate. Furthermore, these molecules are considered GRAS (generally recognised as safe) compounds, except for 2, 4-dihydroxybenzoic acid (24BA).

Vortioxetine (VOT), 1-[2-(2, 4-dimethylphenylsulfanyl) phenyl] piperazine, is a novel antidepressant drug that is used mainly for the treatment of major depressive disorder (MDD) [21,22]. However, because of its low aqueous solubility (0.04 mg/mL in water at 37 °C), it was commercialized in the form of hydrobromide [23]. He et al. [23], Li et al. [24], Zhou et al. [25] and Zhang et al. [26] reported the synthesis of different pharmaceutical solid forms of VOT, and we have previously reported on three straight-chain dicarboxylic acid salt hydrates of VOT [27]. These salt forms could enhance the

solubility of VOT. In this paper, we describe four new dihydroxybenzoic acid salts of VOT, as well as their crystal structures, physicochemical properties, and aqueous solubility. The chemical structures of VOT and dihydroxybenzoic acid are displayed in Scheme 1.



Scheme 1. Chemical structures of vortioxetine and cofomers.

2. Materials and Methods

2.1. Instrumentations and Materials

The corresponding chemicals and reagents were obtained from commercial sources and used without further purification. The differential scanning calorimetry (DSC) analyses were performed on Mettler Toledo DSC2 equipment (Mettler Toledo, Zurich, Switzerland) at a heating rate of 10 °C/min using nitrogen as the purge gas. The thermogravimetric (TGA) analysis of the samples was performed on PerkinElmer TGA 4000 equipment (PerkinElmer, Shanghai, China) with a heating rate of 10 °C/min under a nitrogen gas purge. The X-ray powder diffraction (PXRD) patterns were performed on a German Bruker corporation D8 ADVANCE powder diffractometer (Beijing, China), using a Cu K α radiation tube ($\lambda = 1.5418 \text{ \AA}$, $V = 40 \text{ kV}$ and $I = 40 \text{ mA}$) and the samples were scanned in the 3–60° range. The diffraction data for VOT-23BA-H₂O, VOT-24BA-TOL, and VOT-25BA salts were collected on an Oxford Xcalibur Gemini Ultra diffractometer (Rigaku Oxford Diffraction, Oxford, England) with an Atlas detector operating at 40 kV and 40 mA using Cu K α radiation ($\lambda = 1.54178 \text{ \AA}$), while the other diffraction data for VOT-26BA were performed on a Bruker Apex II CCD diffractometer operating (Bruker, NASDAQ, Germany) at 50 kV and 30 mA using Mo K α radiation ($\lambda = 0.71073 \text{ \AA}$). The corresponding crystal structure was solved by direct methods using the SHELXS program (University of Gottingen, SHELXS-97, Gottingen, Germany) and refined with the SHELXL program (University of Gottingen, SHELXS-97, Gottingen, Germany) [28,29]. Crystallographic parameters and hydrogen bonds are listed in Tables 1 and 2.

2.2. Preparation of Vortioxetine Salts with Dihydroxybenzoic Acids

To prepare VOT-23BA-H₂O (1:1:0.5) salt, vortioxetine (20 mg) (Shanghai Neosun Pharmaceutical Technology Co., Ltd., Shanghai, China) and 23BA (10 mg) (Aladdin, Shanghai, China) were dissolved

in 5 mL of ethanol/water (4:1, v/v) (Aladdin, Shanghai, China), and stirred at room temperature for 1 h. The resulting solution was then left at room temperature to slowly evaporate. The fine block crystals for single crystal X-ray diffraction were found after 15 days.

To prepare VOT-24BA-TOL (1:1:0.5) salt, vortioxetine (20 mg) and 24BA (10 mg) (Aladdin, Shanghai, China) were dissolved in 5 mL of toluene/ethanol (4:1, v/v) (Aladdin, Shanghai, China), and stirred at room temperature for 2 h. The resulting solution was then left at room temperature to slowly evaporate. The fine block crystals for single crystal X-ray diffraction were found after 15 days.

To prepare VOT-25BA (1:1) salt, vortioxetine (20 mg) and 25BA (10 mg) were dissolved in 5 mL of acetone/water (1:1, v/v), and stirred at room temperature for 0.5 h. The resulting solution was then left at room temperature to slowly evaporate. The fine block crystals for single crystal X-ray diffraction were found after seven days.

To prepare VOT-26BA (1:1) salt, vortioxetine (20 mg) and 26BA (10 mg) were dissolved in 6 mL of acetone/water (2:1, v/v), and stirred at room temperature for 2 h. The resulting solution was then left at room temperature to slowly evaporate. The fine needle crystals for single crystal X-ray diffraction were found after seven days.

2.3. Solubility Measurement

The solubility experiments were carried out on a round bottomed flask with a rotation speed of 500 rpm at 37 ± 0.5 °C in aqueous medium. After 24 h, the supernatant was filtered through 0.22 µm nylon filter, and then diluted within the scope of the standard curve with aqueous medium. The concentration of VOT was determined using an Agilent 1290 HPLC system (Agilent, Agilent 1290, Shanghai, China), with a C18 HPLC column (Thermo Accucore aQ 100 × 2.1 mm) (Thermo Fisher, Shanghai, China) and a UV detection wavelength of 226 nm. The column temperature was set at 40 °C, and the mobile phase containing 0.01 mol/L potassium phosphate: acetonitrile (v/v, 60:40) was run at 0.4 mL/min. All of the resulting solution was filtered with 0.22 µm nylon filter and analyzed by the corresponding calibration curve.

Table 1. Crystallographic parameters of vortioxetine and its dihydroxybenzoic acid salts.

	VOT-23BA-H ₂ O	VOT-24BA-TOL	VOT-25BA	VOT-26BA
chemical formula	2C ₁₈ H ₂₃ N ₂ S, 2C ₇ H ₅ O ₄ ,H ₂ O	2C ₁₈ H ₂₃ N ₂ S, 2C ₇ H ₅ O ₄ ,C ₇ H ₈	C ₁₈ H ₂₃ N ₂ S, C ₇ H ₅ O ₄	C ₁₈ H ₂₃ N ₂ S, C ₇ H ₅ O ₄
formula sum	C ₅₀ H ₅₈ N ₄ O ₉ S ₂	C ₅₇ H ₆₄ N ₄ O ₈ S ₂	C ₂₅ H ₂₈ N ₂ O ₄ S	C ₂₅ H ₂₈ N ₂ O ₄ S
formula weight	923.12	997.24	452.55	452.55
crystal system	monoclinic	triclinic	triclinic	monoclinic
space group	C2/c	P-1	P-1	P21/c
<i>a</i> (Å)	26.5624(5)	12.3577(8)	9.9394(8)	17.0666(8)
<i>b</i> (Å)	8.10730(10)	12.9526(6)	10.1982(6)	6.3133(2)
<i>c</i> (Å)	23.0375(5)	17.4064(11)	12.1724(9)	22.2716(10)
<i>A</i> (°)	90	82.219(5)	89.628(6)	90
<i>B</i> (°)	92.162(2)	80.757(6)	76.453(7)	107.112(5)
<i>γ</i> (°)	90	87.213(4)	85.399(6)	90
<i>Z</i>	4	2	2	4
<i>V</i> (Å ³)	4957.58(16)	2723.6(3)	1195.55(15)	2293.46(17)
<i>D</i> _{calc} (g cm ⁻³)	1.237	1.216	1.257	1.311
<i>M</i> (mm ⁻¹)	1.444	1.339	1.472	0.175
reflns. collected	4385	9612	4573	3075
observed reflns.	3509	3889	2187	2592
<i>R</i> ₁ (<i>I</i> > 2σ (<i>I</i>))	0.0438	0.0677	0.0632	0.0409
w <i>R</i> ₂ (all data, <i>F</i> ²)	0.1246	0.1703	0.1704	0.0995
GOF	1.054	1.036	1.042	1.013
largest diff. peak and hole (e·Å ⁻³)	0.775/−0.168	0.341/−0.356	0.271/−0.468	0.184/−0.240
CCDC	1,937,936	1,937,937	1,937,938	1,937,939

Table 2. Hydrogen bond distances (Å) and angles (°) of vortioxetine and its dihydroxybenzoic acid salts.

H-Bond	d(D–H)	d(H…A)	d(D…A)	∠(DHA)	Symmetry Code
VOT-23BA-H ₂ O					
N1 ⁺ –H1B…O3	0.88	1.99	2.856(2)	166	x, y, z
N1 ⁺ –H1A…O5	0.93	1.86	2.783(2)	174	x, y, z
O3–H3…O2	1.01	1.51	2.471(2)	156	x, y, z
O4–H4…O1	0.88	1.71	2.585(2)	177	x, y+1, z
O5–H5A…O2	0.90	1.77	2.658(2)	172	x, y+1, z
VOT-24BA-TOL					
N1 ⁺ –H1C…O1	0.80	2.02	2.804(4)	165	-x+1, -y+1, -z
N1 ⁺ –H1D…O2	1.04	1.70	2.722(4)	167	x, y+1, z
N3 ⁺ –H3C…O6	0.86	1.88	2.738(4)	168	x-1, y, z
N3 ⁺ –H3D…O5	0.93	1.82	2.743(4)	170	-x+1, -y+1, -z
O3–H3…O2	0.92	1.67	2.542(4)	155	x, y, z
O4–H4…O5	0.70	2.04	2.726(4)	169	x, y, z
O7–H7A…O6	0.76	1.81	2.526(4)	155	x, y, z
O8–H8A…O1	0.93	1.79	2.714(4)	171	x, y+1, z
VOT-25BA					
N1 ⁺ –H1C…O2	0.97	1.86	2.810(3)	168	x, y+1, z
N1 ⁺ –H1D…O1	1.01	1.72	2.723(3)	173	-x, -y+1, -z
O3–H3…O1	0.96	1.68	2.555(3)	150	x, y, z
O4–H4…O2	0.89	1.84	2.685(3)	157	-x+1, -y, -z
VOT-26BA					
N1 ⁺ –H1A…O2	0.91	1.91	2.814(3)	173	-x+1, y-1/2, -z+3/2
N1 ⁺ –H1B…O1	0.95	1.85	2.753(3)	158	x, -y-1/2, z-1/2
O3–H3…O2	0.82	1.82	2.548(3)	147	x, y, z
O4–H4…O1	0.82	1.85	2.573(3)	147	x, y, z

3. Results and Discussion

3.1. Crystal Structure Analysis

3.1.1. Crystal Structure of VOT-23BA-H₂O (1:1:0.5) Salt

The VOT-23BA-H₂O salt crystallized in the monoclinic space group C2/c with one VOT cation, one 23BA anion, and one half water molecule in the asymmetric unit. In the VOT-23BA-H₂O salt, each water molecule interacted with two 23BA anions to form a two-dimensional plane structure along the crystallographic ab plane through O4–H4…O1 and O5–H5A…O2 hydrogen bonds (Figure 1a). The aforementioned plane structures and VOT cations were arranged in a sandwich 3D structure via N1⁺–H1B…O3 and N1⁺–H1A…O5 hydrogen bonds (Figure 1b).

3.1.2. Crystal Structure of VOT-24BA-TOL (1:1:0.5) Salt

The VOT-24BA-TOL salt crystallized in the triclinic space group P-1 with two VOT cations, two 24BA anions, and one toluene molecule in the asymmetric unit. In the VOT-24BA-TOL salt, two different 24BA anions interacted with each other to form a one-dimensional chain structure through O4–H4…O5 and O8–H8A…O1 hydrogen bonds (Figure 2a). The aforementioned chain structures and VOT cations were arranged in a complex three-dimensional structure via N1⁺–H1C…O1, N1⁺–H1D…O2, N3⁺–H3C…O6, and N3⁺–H3D…O5 hydrogen bonds (Figure 2b). In addition, the toluene molecules existed in the cavity of VOT-24BA-TOL salt along the crystallographic a-axis (Figure 2c).

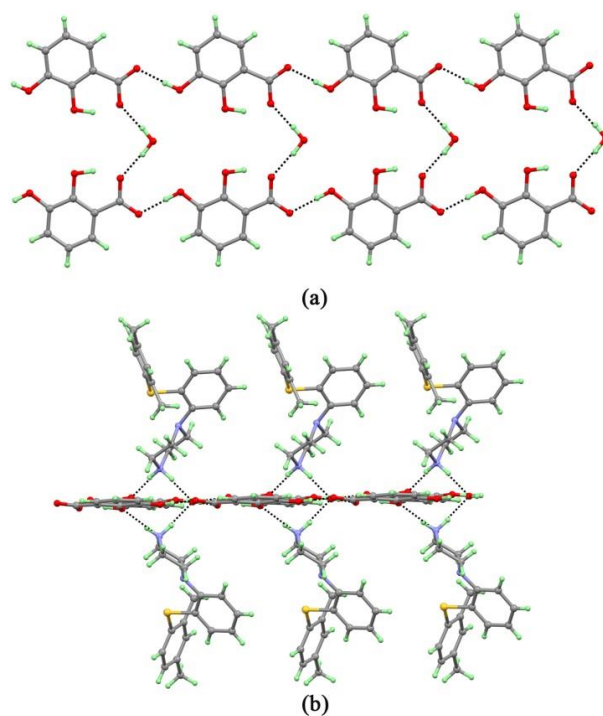


Figure 1. (a) Two 23BA anions and one water molecule form a two-dimension plane structure along the crystallographic b-axis through O4–H4···O1 and O5–H5A···O2 hydrogen bonds; (b) the sandwich 3D structure of the VOT-23BA-H₂O salt.

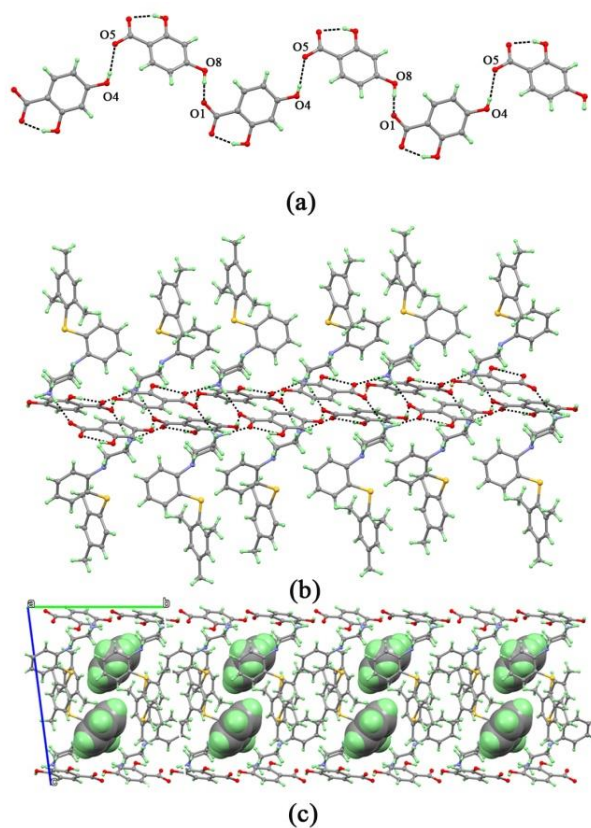


Figure 2. (a) Two 24BA anions interacted with each other to form a one-dimensional chain structure. (b) The complex 3D structure of the VOT-24BA-TOL salt. (c) The toluene molecules existed in the cavity of the VOT-24BA-TOL salt.

3.1.3. Crystal Structure of VOT-25BA (1:1) Salt

The VOT-25BA salt crystallized in the triclinic space group P-1 with one VOT cation and one 25BA anion in the asymmetric unit. In the VOT-25BA salt, two 25BA molecules interacted with each other to form an $R_2^2(14)$ synthon through O4–H4···O2 hydrogen bonds (Figure 3a). The aforementioned $R_2^2(14)$ synthons and VOT cations were arranged in a sandwich $R_4^4(12)$ structure via $N1^+–H1C···O2$ and $N1^+–H1D···O1$ hydrogen bonds (Figure 3b).

3.1.4. VOT-26BA (1:1) Salt

The VOT-26BA salt crystallized in the monoclinic space group P21/c with one VOT cation and one 26BA anion in the asymmetric unit. In the VOT-26BA salt, two VOT cations and two 26BA anions formed a [2+2] tetrameric $R_4^4(12)$ synthon via $N1^+–H1A···O2$ and $N1^+–H1B···O1$ hydrogen bonds (Figure 4).

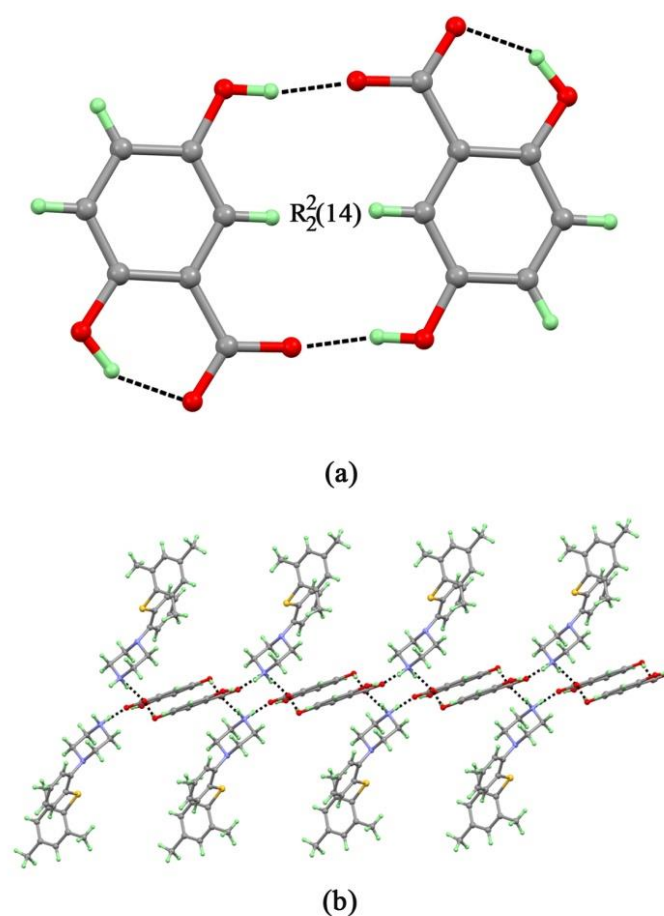


Figure 3. (a) Two 25BA anions formed an $R_2^2(14)$ synthon through O4–H4···O2 hydrogen bonds. (b) The sandwich 3D structure of the VOT-25BA salt.

3.1.5. Structural Comparison

The spatial variation of similar structures is important for the study of packing similarities. As shown in Scheme 2, there is no classical hydrogen bonding in pure VOT. VOT-24BA-TOL, VOT-25BA, and VOT-26BA shared similar [2+2] tetrameric $R_4^4(12)$ hydrogen bonds. However, because the locations of the two hydroxyl groups changed, they showed the different space-stacked structures after salting (Figure S1). Specifically, the VOT molecules of the VOT-23BA-H₂O salt were linked by protonated piperazine-hydroxyl N–H···O hydrogen bonds, not protonated piperazine-deprotonated carboxylic acid N–H···O hydrogen bonds, involving the hydroxyl groups.

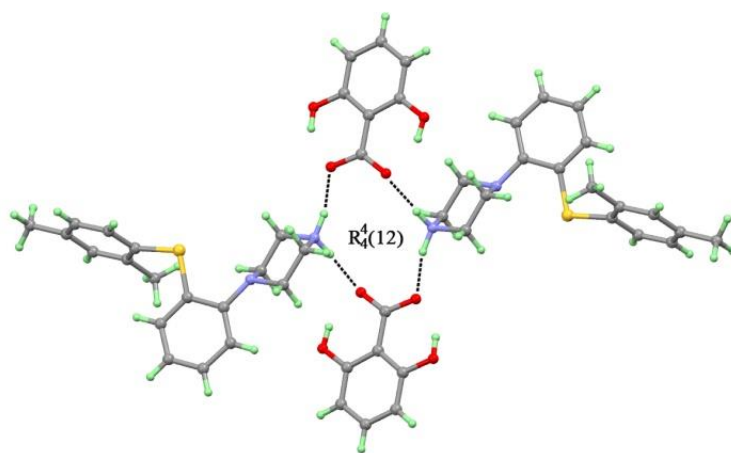
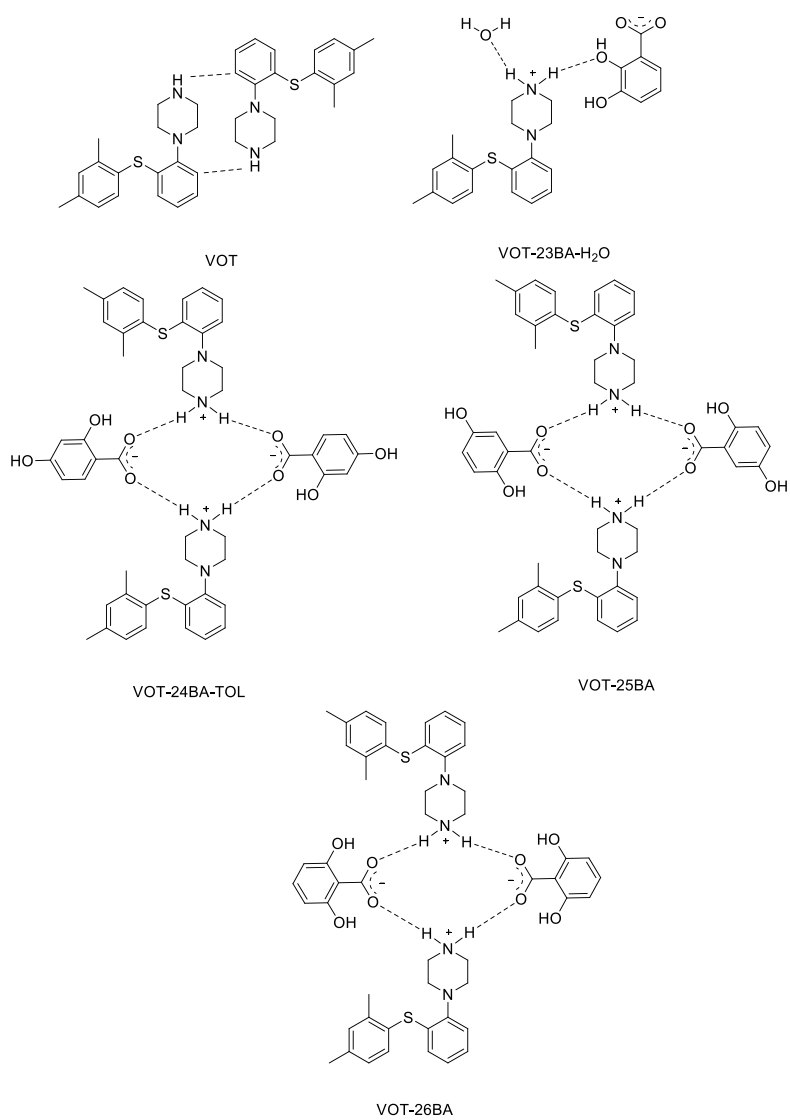


Figure 4. The [2+2] tetrameric structure in the VOT-26BA salt.



Scheme 2. Different hydrogen bonds synthons in crystal structures.

3.2. Powder X-ray Diffraction Analyses

Powder X-ray diffraction (PXRD) is one of the important tools to differentiate phase transition. The PXRD patterns for VOT, VOT-23BA-H₂O, VOT-24BA-TOL, VOT-25BA, and VOT-26BA salts are shown in Figure 5 and Figures S2–S5 (Supporting Information). VOT showed major characteristic peaks at $2\theta = 11.6^\circ, 12.34^\circ, 12.80^\circ, 14.32^\circ, 15.12^\circ, 16.84^\circ, 17.40^\circ, 18.62^\circ, 19.06^\circ, 20.48^\circ, 21.50^\circ, 22.48^\circ, 22.96^\circ, 24.38^\circ, 25.66^\circ,$ and 26.18° . However, the VOT-23BA-H₂O, VOT-24BA-TOL, VOT-25BA, and VOT-26BA salts exhibited different characteristic peaks, which indicate the formation of new solid forms (Table S1).

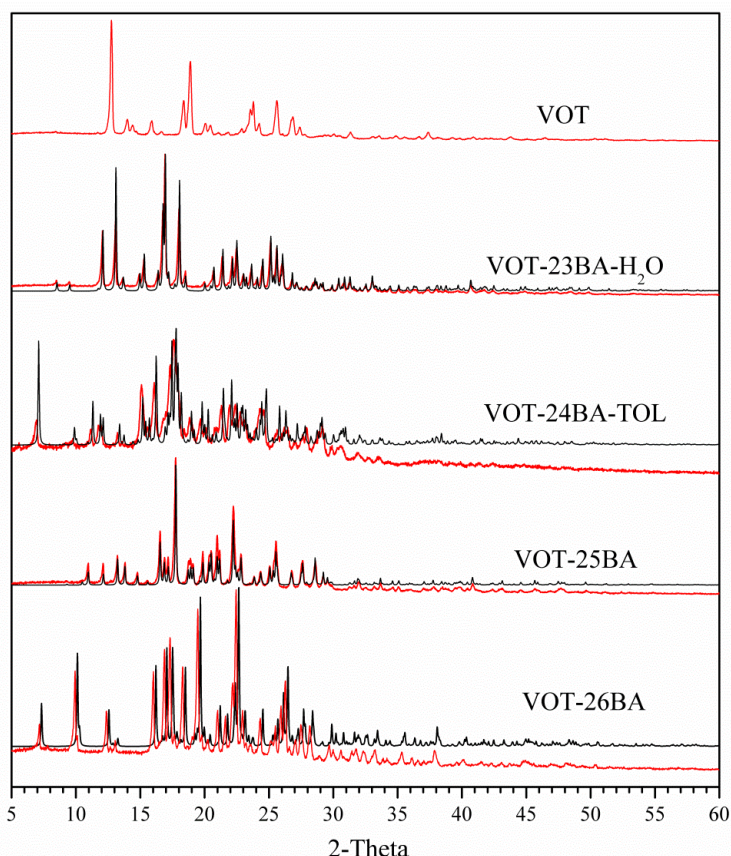


Figure 5. Experimental (red) and simulated (black) powder X-ray diffraction (PXRD) patterns for VOT, VOT-23BA-H₂O, VOT-24BA-TOL, VOT-25BA, and VOT-26BA salts.

3.3. Thermal Analyses

Vortioxetine and its salts were investigated by DSC and TGA, and the corresponding profiles are shown in Figure 6. The DSC thermogram of vortioxetine exhibited a single melting endothermic peak at 117°C , which was attributed to the melting process, and its TGA curve showed that vortioxetine had no weight loss before decomposition at 226°C (Figure 6a).

The DSC thermogram of VOT-23BA-H₂O showed an endothermic peak at 163°C , accompanied by a mass loss of 2.28% in the TGA curve at $140\text{--}173^\circ\text{C}$, which indicates that VOT-23BA-H₂O released half a water molecule per VOT-23BA-H₂O (theoretical value: 1.95%), followed by a melting endothermic peak at 198°C . Then, a broad endothermic peak at 232°C was observed in the DSC curve, which is attributable to decomposition behavior (Figure 6b), and the TGA curve also revealed a uniform degradation process at 200°C .

The DSC thermogram of VOT-24BA-TOL showed a broad endothermic peak at 158°C , and the TGA curve of VOT-24BA-TOL began to decompose at 115°C (the onset temperature of the degradation curve), indicating a process of simultaneous melting and decomposition; these data suggest poor thermodynamic stability of VOT-24BA-TOL in environmental conditions. Furthermore, the DSC and

TGA analyses of VOT-24BA-TOL showed that the simultaneous melting and decomposition process was non-reversible, which means that desolvation experiments were difficult to carry out through either simple heat or vacuum drying.

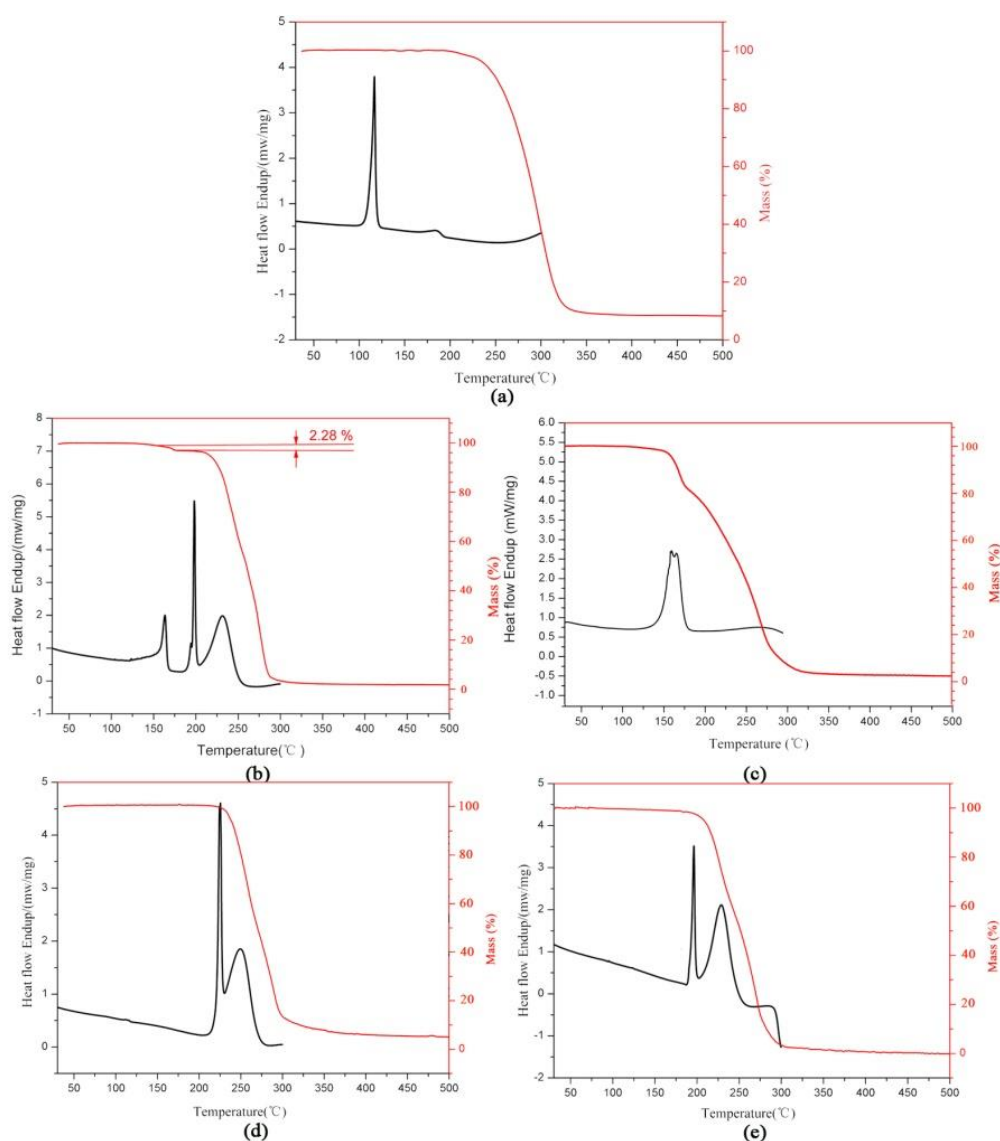


Figure 6. DSC (black) and TGA (red) curves of VOT and its salts: (a) VOT, (b) VOT-23BA-H₂O, (c) VOT-24BA-TOL, (d) VOT-25BA, and (e) VOT-26BA.

The DSC thermogram of VOT-25BA exhibited a sharp endothermic peak at 224 °C, and the TGA curve of VOT-25BA began to decompose at 206 °C, indicating that the melting process was accompanied by the decomposition process.

The DSC thermogram of VOT-26BA exhibited a sharp endothermic peak at 197 °C, and the TGA curve of VOT-26BA began to decompose at 184 °C, indicating that it was also a process of simultaneous melting and decomposition. The results of the DSC curves indicate that all the salts showed higher physical stability than the pure VOT.

3.4. Aqueous Solubility and Stability study

Aqueous solubility is an important property for drug oral activity as well as for pharmaceutical preparation [30]. The solubility study of vortioxetine and its dihydroxybenzoic salts were determined in water at 37 °C. The powder samples of the undissolved residue were also analyzed via PXRD,

and the results showed that VOT-23BA-H₂O, VOT-25BA, and VOT-26BA remained stable in water after 24-h solubility experiments (Figures S6–S10), while the VOT-24BA-TOL salt was unstable in aqueous solution. Furthermore, a simple comparison of the residual materials after solubility experiments with the patterns of former compounds (VOT and 24BA) is shown in Figure S11 and Table S2, the results showed a significant difference among the residual material, VOT and 24BA. This implies that the VOT-24BA-TOL was not resolved into VOT and 24BA, but rather an irreversible process. The solubility of dihydroxybenzoic salts followed the order of VOT-25BA > VOT-26BA > VOT-23BA-H₂O (Table 3). In aqueous medium, the VOT-23BA-H₂O, VOT-25BA, and VOT-26BA salts were found to more soluble than pure VOT.

Table 3. Solubility of vortioxetine and its dihydroxybenzoic acid salts in water at 37 °C.

Compound	Equilibrium Solubility of VOT in Water (mg/mL)	Coformer Solubility in Water ^(a) (mg/mL)
VOT	0.04	-
VOT-23BA-H ₂ O	0.09	26.10
VOT-24BA-TOL	-	5.78
VOT-25BA	0.35	5.00
VOT-26BA	0.20	9.56

(a) Data source: ChemIDplus Advanced (<http://www.chem.sis.nlm.nih.gov/chemidplus/>).

4. Conclusions

In summary, four dihydroxybenzoic acid salts of the antidepressant drug vortioxetine were synthesized by slow solvent evaporation crystallization. VOT-24BA-TOL, VOT-25BA, and VOT-26BA showed similar [2+2] tetrameric R₄⁴ (12) hydrogen bonds by acid-piperazine heterosynthon, whereas in the VOT-23BA-H₂O salt, the VOT cation and 23BA anion interacted through protonated piperazine-hydroxyl N-H...O hydrogen bonds, not protonated piperazine-deprotonated carboxylic acid N-H...O hydrogen bonds. The DSC results indicate that all the salts showed higher physical stability than the pure VOT. The solubility study revealed that the VOT-23BA-H₂O, VOT-25BA, and VOT-26BA salts exhibited an increased solubility in water compared to pure VOT. Furthermore, 25BA is considered a GRAS molecule and the solubility data indicate that the VOT-25BA salt may be a promising drug candidate.

Supplementary Materials: The following are available online at <http://www.mdpi.com/2073-4352/9/10/536/s1>, Figure S1: The different space stacked structure of VOT, VOT-23BA-H₂O, VOT-24BA-TOL, VOT-25BA and VOT-26BA salts; Figure S2: Experimental (red) and simulated (black) PXRD patterns for VOT-23BA-H₂O salt; Figure S3: Experimental (red) and simulated (black) PXRD patterns for VOT-24BA-TOL salt; Figure S4: Experimental (red) and simulated (black) PXRD patterns for VOT-25BA salt; Figure S5: Experimental (red) and simulated (black) PXRD patterns for VOT-26BA salt; Figure S6: PXRD analysis of the residual materials of VOT after 24h solubility in aqueous medium; Figure S7: PXRD analysis of the residual materials of VOT-23BA-H₂O after 24h solubility in aqueous medium; Figure S8: PXRD analysis of the residual materials of VOT-24BA-TOL after 24h solubility in aqueous medium; Figure S9: PXRD analysis of the residual materials of VOT-25BA after 24h solubility in aqueous medium; Figure S10: PXRD analysis of the residual materials of VOT-26BA after 24h solubility in aqueous medium; Figure S11: The comparison diagram of the residual materials of VOT-24BA-TOL after 24h solubility with the patterns of former compounds (VOT and 24BA); Table S1: The major PXRD peaks (2θ) for VOT, VOT-23BA-H₂O, VOT-24BA-TOL, VOT-25BA and VOT-26BA salts; Table S2: The major PXRD peaks (2θ) for the residual materials of VOT-24BA-TOL, VOT and 24BA.

Author Contributions: C.-J.C. and X.-R.Z. conceived and designed the experiments; L.G. and G.-Y.H. performed the experiments and analyzed the data. All the authors contributed to manuscript revision.

Funding: This research was funded by National Natural Science Foundation, grant number 81860736 and Guangxi Natural Science Foundation, grant number 2018GXNSFBA281167.

Acknowledgments: The work was supported by National Natural Science Foundation (Grant No.: 81860736) and Guangxi Natural Science Foundation (Grant No.: 2018GXNSFBA281167).

Conflicts of Interest: The authors declare no conflict of interest.

References

1. Owoyemi, B.C.D.; da Silva, C.C.P.; Souza, M.S.; Diniz, L.F.; Ellena, J.; Carneiro, R.L. Synthesis and structural characterization of four new pharmaceutical cocrystal forms. *Cryst. Growth Des.* **2019**, *5*, 648–657. [[CrossRef](#)]
2. Nechipadappu, S.K.; Trivedi, D.R. Pharmaceutical salts of ethionamide with GRAS counter ion donors to enhance the solubility. *Eur. J. Pharm. Sci.* **2017**, *96*, 578–589. [[CrossRef](#)] [[PubMed](#)]
3. Berge, S.M.; Bighley, L.D.; Monkhouse, D.C. Pharmaceutical salts. *J. Pharm. Sci.* **1977**, *66*, 1–19. [[CrossRef](#)] [[PubMed](#)]
4. Morissette, S.L.; Almarsson, O.; Peterson, M.L.; Remenar, J.F.; Read, M.J.; Lemmo, A.V.; Ellis, S.; Cima, M.J.; Gardner, C.R. High-throughput crystallization: Polymorphs, salts, co-crystals and solvates of pharmaceutical solids. *Adv. Drug Deliver. Rev.* **2004**, *56*, 275–300. [[CrossRef](#)] [[PubMed](#)]
5. Liu, L.; Zou, D.; Zhang, Y.; Zhang, D.; Zhang, Y.; Zhang, Q.; Wang, J.; Zeng, S.; Wang, C. Assembly of three pharmaceutical salts/cocrystals of tetrahydroberberine with sulfophenyl acids: Improving the properties by formation of charge-assisted hydrogen bonds. *New J. Chem.* **2019**, *43*, 4886–4894. [[CrossRef](#)]
6. Carvalho, P.S.; Diniz, L.F.; Tenorio, J.C.; Souza, M.S.; Franco, C.H.; Rial, R.C.; de Oliveira, K.R.W.; Nazario, C.E.D.; Ellena, J. Pharmaceutical paroxetine-based organic salts of carboxylic acids with optimized properties: The identification and characterization of potential novel API solid forms. *CrystEngComm* **2019**, *21*, 3668–3678. [[CrossRef](#)]
7. Sathisaran, I.; Dalvi, S. Engineering cocrystals of poor water-soluble drugs to enhance dissolution in aqueous medium. *Pharmaceutics* **2018**, *10*, 108. [[CrossRef](#)]
8. Owoyemi, B.C.D.; Da Silva, C.C.P.; Diniz, L.F.; Souza, M.S.; Ellena, J.; Carneiro, R.L. Fluconazolium oxalate: Synthesis and structural characterization of a highly soluble crystalline form. *CrystEngComm* **2019**, *21*, 1114–1121. [[CrossRef](#)]
9. Arabiani, M.R.; Lodagekar, A.; Yadav, B.; Chavan, R.B.; Shastri, N.R.; Purohit, P.Y.; Shelat, P.; Dave, D. Mechanochemical synthesis of brexpiprazole cocrystals to improve its pharmaceutical attributes. *CrystEngComm* **2019**, *21*, 800–806. [[CrossRef](#)]
10. Park, B.; Yoon, W.; Yun, J.; Ban, E.; Yun, H.; Kim, A. Emodin-nicotinamide (1:2) cocrystal identified by thermal screening to improve emodin solubility. *Int. J. Pharm.* **2019**, *557*, 26–35. [[CrossRef](#)]
11. Lu, Q.; Dun, J.; Chen, J.M.; Liu, S.; Sun, C.C. Improving solid-state properties of berberine chloride through forming a salt cocrystal with citric acid. *Int. J. Pharm.* **2019**, *554*, 14–20. [[CrossRef](#)]
12. Burchell, C.J.; Ferguson, G.; Lough, A.J.; Gregson, R.M.; Glidewell, C. Hydrated salts of 3,5-dihydroxybenzoic acid with organic diamines: Hydrogen-bonded supramolecular structures in two and three dimensions. *Acta Crystallogr. B* **2001**, *57*, 329–338. [[CrossRef](#)] [[PubMed](#)]
13. Childs, S.L.; Hardcastle, K.I. Cocrystal of chlorzoxazone with carboxylic acids. *CrystEngComm* **2007**, *9*, 364–367. [[CrossRef](#)]
14. Brittain, H.G. Cocrystal systems of pharmaceutical interest: 2010. *Cryst. Growth Des.* **2012**, *12*, 1046–1054. [[CrossRef](#)]
15. Sanphui, P.; Tothadi, S.; Ganguly, S.; Desiraju, G.R. Salt and cocrystals of sildenafil with dicarboxylic acids: Solubility and pharmacokinetic advantage of the glutarate salt. *Mol. Pharm.* **2013**, *10*, 4687–4697. [[CrossRef](#)] [[PubMed](#)]
16. Varughese, S.; Desiraju, G.R. Using water as a design element in crystal engineering. Host-guest compounds of hydrated 3,5-dihydroxybenzoic acid. *Cryst. Growth Des.* **2010**, *10*, 4184–4196. [[CrossRef](#)]
17. Gautam, M.K.; Besan, M.; Pandit, D.; Mandal, S.; Chadha, R. Cocrystal of 5-fluorouracil: Characterization and evaluation of biopharmaceutical parameters. *AAPS PharmSciTech* **2019**, *20*, 149. [[CrossRef](#)]
18. Barbas, R.; Font-Bardia, M.; Paradkar, A.; Hunter, C.A.; Prohens, R. Combined virtual/experimental multicomponent solid forms screening of sildenafil: New salts, cocrystals, and hybrid salt-cocrystals. *Cryst. Growth Des.* **2018**, *18*, 7618–7627. [[CrossRef](#)]
19. Nechipadappu, S.K.; Reddy, I.R.; Tarafder, K.; Trivedi, D.R. Salt/cocrystal of anti-fibrinolytic hemostatic drug tranexamic acid: Structural, DFT, and stability study of salt/cocrystal with GRAS molecules. *Cryst. Growth Des.* **2018**, *19*, 347–361. [[CrossRef](#)]
20. Bora, P.; Saikia, B.; Sarma, B. Regulation of $\pi\cdots\pi$ stacking interactions in small molecule cocrystals and/or salts for physicochemical property modulation. *Cryst Growth Des.* **2018**, *18*, 1448–1458. [[CrossRef](#)]

21. Sanchez, C.; Asin, K.E.; Artigas, F. Vortioxetine, a novel antidepressant with multimodal activity: Review of preclinical and clinical data. *Pharmacol. Ther.* **2015**, *145*, 43–57. [[CrossRef](#)] [[PubMed](#)]
22. McIntyre, R.S.; Lophaven, S.; Olsen, C.K. A randomized, double-blind, placebo-controlled study of vortioxetine on cognitive function in depressed adults. *Int. J. Neuropsychop.* **2014**, *17*, 1557–1567. [[CrossRef](#)] [[PubMed](#)]
23. He, S.F.; Zhang, X.R.; Zhang, S.; Guan, S.; Li, J.; Li, S.; Zhang, L. An investigation into vortioxetine salts: Crystal structure, thermal stability, and solubilization. *J. Pharm. Sci.* **2016**, *105*, 2123–2128. [[CrossRef](#)] [[PubMed](#)]
24. Li, J.; Li, L.Y.; He, S.F.; Li, S.; Dong, C.Z.; Zhang, L. Crystal structures, X-ray photoelectron spectroscopy, thermodynamic stabilities, and improved solubilities of 2-hydrochloride salts of vortioxetine. *J. Pharm. Sci.* **2017**, *106*, 1069–1074. [[CrossRef](#)] [[PubMed](#)]
25. Zhou, X.; Hu, X.; Wu, S.; Ye, J.; Sun, M.; Gu, J.; Zhu, J.; Zhang, Z. Structures and physicochemical properties of vortioxetine salts. *Acta Crystallogr. B* **2016**, *72*, 723–732. [[CrossRef](#)] [[PubMed](#)]
26. Zhang, S.; Zhang, X.R.; He, S.F.; Li, J.; Zhang, L. Syntheses, crystal structures and theoretical studies of three novel salts of vortioxetine and the investigation of their solubility. *Chin. J. Struct. Chem.* **2016**, *35*, 1645–1654.
27. Gao, L.; Zhang, X.R.; Yang, S.P.; Liu, J.J.; Chen, C.J. Improved solubility of vortioxetine using C2–C4 straight-chain dicarboxylic acid salt hydrates. *Crystals* **2018**, *8*, 352. [[CrossRef](#)]
28. Sheldrick, G.M. *SHELXTL, Version 5.1*; Bruker Analytical X-ray Instruments Inc.: Madison, WI, USA, 1998.
29. Sheldrick, G.M. *SHELXL-97, PC Version*; University of Göttingen: Göttingen, Germany, 1997.
30. Lipinski, C. Poor aqueous solubility—An industry wide problem in drug discovery. *Am. Pharm. Rev.* **2002**, *5*, 82–85.



© 2019 by the authors. Licensee MDPI, Basel, Switzerland. This article is an open access article distributed under the terms and conditions of the Creative Commons Attribution (CC BY) license (<http://creativecommons.org/licenses/by/4.0/>).